Inorg. Chem. **2008**, *47*, 8179−8187

Self-Assembly of Polyoxometalate-Based Metal Organic Frameworks Based on Octamolybdates and Copper-Organic Units: from Cu^{II}, $Cu^{I,II}$ to Cu^{I} via Changing Organic Amine

Ya-Qian Lan, Shun-Li Li, Xin-Long Wang, Kui-Zhan Shao, Dong-Ying Du, Hong-Ying Zang, and Zhong-Min Su*

Institute of Functional Material Chemistry; Key Laboratory of Polyoxometalate Science of Ministry of Education, Faculty of Chemistry, Northeast Normal University, Changchun 130024, China

Received April 19, 2008

Six polyoxometalate (POM)-based hybrid materials have been designed and synthesized based on octamolybdate building blocks and copper-organic units at different pH values under hydrothermal conditions, namely, $[H_2bbi][Cu^{II}(bbi)_2(\beta\text{-}Mo_8O_{26})]$ (**1**), $[Cu^{II}(bbi)_2(H_2O)(\beta\text{-}Mo_8O_{26})_{0.5}]$ (**2**), $[Cu^{II}(bbi)_2(\alpha\text{-}Mo_8O_{26})][Cu^{I}(bbi)]_2$ (**3**), $[Cu^{II}Cu^{I}(bbi)_3(\alpha\text{-}Mo_8O_{26})][Cu^{I}(bbi)]$ (**4**), $[Cu^{I}(bbi)]_2[Cu^{I}_2(bbi)_2(\delta\text{-}Mo_8O_{26})_{0.5}][\alpha\text{-}Mo_8O_{26}]_{0.5}$ (**5**), and $[Cu^{I}(bbi)][Cu^{I}(bbi)(\theta\text{-}Mo_8O_{26})_{0.5}]$ (**6**), where bbi is 1,1′-(1,4-butanediyl)bis(imidazole). Their crystal structures have been determined by X-ray diffraction. In compound **1**, the bbi ligands with bis-monodentate coordination modes link Cu^{II} cations to generate a 2D copper-organic unit with (4, 4) net, which is pillared by the $(\beta\text{-}Mo_8O_{26})^{4-}$ anions to form a 3D framework with α-Po topology. The similar copper-organic units are connected alternately by $(\beta\text{-}Mo_8O_{26})^{4-}$ anions to generate a 3D 2-fold interpenetrating (4,6)-connected framework with $(4^4\cdot6^2)(4^4\cdot6^{10}\cdot8)$ topology in compound **2**. Compounds **3** and **4** are supramolecular isomers with polythreaded topology. If $Cu^{I}\cdots O$ interactions are considered, the structure of **3** is a novel self-penetrating (3,4,6)-connected framework with $(5^2\cdot8)_2(5^4\cdot6\cdot8)(4^4\cdot6^{10}\cdot10)$ topology, and the structure of **4** is a (4,6)-connected framework with $(4^2\cdot6^3\cdot7)(5\cdot6^4\cdot8)(4^2\cdot5^6\cdot6^6\cdot8)(4^2\cdot5^6\cdot6^4\cdot7\cdot8^2)$ topology. Different from compounds **3** and **4**, compounds **5** and **6** are supramolecular isomers with polythreaded topology based on different octamolybdate isomers. By careful inspection of the structures of **1**−**6**, it is believed that various copper-organic units, which are formed by bbi ligands combined with Cu^{II}/Cu^{I} cations, octamolybdates with different types and coordination modes, and the nonbonding interactions between polyanions and copper-organic units are important for the formation of the different structures. In addition, with step by step increasing of the amount of organic amine, we have achieved the transformation of Cu^{II} ions into Cu^{I} ones in different degrees in POMs-based metal-organic frameworks (MOFs) for the first time. The infrared spectra, X-ray powder diffraction, and thermogravimetric analyses have been investigated in detail for all compounds, and the luminescent properties have been also been investigated for compounds **3** and **4**.

Introduction

Hybrid inorganic−organic compounds are a new generation of solid-state materials that have promising applications in gas storage, catalysis, and porous materials owing to their chemical and structural diversities.[1] Polyoxometalates (POMs),[2] a unique class of metal-oxide clusters, have many properties that make them attractive for applications in medicine, biology, magnetism, materials science, and catalysis.[3] They cover an enormous range in size and structure and thereby provide access to a huge library of readily available and controllable second building units (SBUs).[4] Recently presented, a remarkable approach for constructing metal-organic frameworks (MOFs) with desired properties is the use of the coordination ability of polyanions to combine with different transition-metal organic units.[5] This method may bring together the merits of each, such as structural diversity with unique framework topologies and the combination of the unique physical and chemical properties of POMs with the features of MOFs.[6]

* To whom correspondence should be addressed. E-mail: zmsu@nenu.edu.cn. Phone: +86 431 85099108.

10.1021/ic800702d CCC: $40.75
Published on Web 08/13/2008

Recently, in situ metal/ligand reactions have been presented in coordination polymers which may serve as a new bridge between coordination chemistry and synthetic organic chemistry.[7] Some in situ ligand syntheses including dehydrogenative carbon−carbon coupling, hydroxylation of aromatic rings, cycloaddition of organic nitriles with azide and ammonia, and transformation of inorganic and organic sulfur have been developed toward construction of novel MOF materials by using a copper(II)-mediated process.[7a] Cu^{II} can be easily converted into Cu^{I} in the presence of different types of aromatic species.[8] Chen and co-workers have performed prominent work and reviewed these kinds of reactions.[7a] With step by step increase of the temperature and the amount of aqueous ammonia, they have successfully synthesized a series of polymeric Cu^{II}, mixed-valent $Cu^{I,II}$ and Cu^{I} imidazolates exhibiting intriguing structures.[9] Additionally, a few POM-based MOFs have successfully been assembled based on copper-organic units,[5c,d,h] but the detailed investigation on the transformation reduction of Cu^{II} ions into Cu^{I} ones in different degrees has not been reported in POM-based MOFs.

Supramolecular isomerism can be a consequence of the effect of the same molecular components generating different supramolecular synthons and could be synonymous with polymorphism.[10] The design of a molecular building block for supramolecular isomers with a fixed chemical stoichiometry is difficult since many factors can influence the composition.[11] Therefore, the synthesis of supramolecular isomers should be regarded as a significant research topic in crystal engineering and in understanding the structure−property relationship of MOFs. A variety of supramolecular isomers, such as the zero-dimensional ring, 1D zigzag, helical chains, and high-membered polygons, have successfully been assembled by angular and linear building blocks.[10a,7b] However, there is an unfavorable investigation on supramolecular isomerism in POM-based MOFs. Up to now, only a limited number of POMs-based supramolecular isomers have been observed in MOFs.[12]

As shown above, it is a great challenge not only to synthesize the supramolecular isomers in POM-based MOFs but also to achieve the transformation of Cu^{II} ions into Cu^{I} ones in different degrees in the above-mentioned system. To achieve this aim, several factors must be taken into account, such as the coordination geometry of metal ions (Cu^{II} or Cu^{I} ions), the nature of organic ligands, the variety of POMs, and the topological and geometrical relations between the copper ions and the ligand. In our strategy, octamolybdate, flexible ligand 1,1′-(1,4-butanediyl)bis(imidazole) (bbi), copper nitrate and Et_3N were chosen based on the following considerations: (i) The selection of the reducer plays a crucial role in the transformation of Cu^{II} ions into Cu^{I} ones. The Cu^{II} cations can be reduced to Cu^{I} cations by organic amine

(1) (a) Cheetham, A. K.; Rao, C. N. R.; Feller, R. K. *Chem. Commun.* **2006**, 4780. (b) Rowsell, J. L. C.; Millward, A. R.; Park, K. S.; Yaghi, O. M. *J. Am. Chem. Soc.* **2004**, *126*, 5666. (c) Rowsell, J. L. C.; Yaghi, O. M. *Angew. Chem., Int. Ed.* **2005**, *44*, 4670. (d) Rood, J. A.; Noll, B. C.; Henderson, K. W. *Inorg. Chem.* **2006**, *45*, 5521. (e) Spencer, E. C.; Howard, J. A. K.; Mclntyre, G. J.; Rowsell, J. L. C.; Yaghi, O. M. *Chem. Commun.* **2006**, 278. (f) Fujita, M.; Kwon, Y. J.; Washizu, S.; Ogura, K. *J. Am. Chem. Soc.* **1994**, *116*, 1151. (g) Wu, C.-D.; Hu, A.; Zhang, L.; Lin, W.-B. *J. Am. Chem. Soc.* **2005**, *127*, 8940. (h) Clearfield, A.; Wang, Z.-K. J. *Chem. Soc., Dalton Trans.* **2002**, 2937. (i) Holman, K. T.; Pivovar, A. M.; Swift, J. A.; Ward, M. D. *Acc. Chem. Res.* **2001**, *34*, 107. (j) Pan, L.; Olson, D. H.; Ciemnolonski, L. R.; Heddy, R.; Li, J. *Angew. Chem., Int. Ed.* **2006**, *45*, 616. (k) Kitagawa, S.; Kitaura, R.; Noro, S. *Angew. Chem., Int. Ed.* **2004**, *43*, 2334. (l) Sun, Y.-Q.; Zhang, J.; Chen, Y.-M.; Yang, G.-Y. *Angew. Chem., Int. Ed.* **2005**, *44*, 5814.

(2) (a) Pope, M. T. *Heteropoly and Isopoly Oxometalates*; Springer: Berlin, 1983. (b) Wu, C.-D.; Lu, C.-Z.; Zhuang, H.-H.; Huang, J.-S. *J. Am. Chem. Soc.* **2002**, *124*, 3836. (c) Hill, C. L. *Chem. Rev.* **1998**, *98*, 1. (d) Khan, M. I.; Yohannes, E.; Doedens, R. J. *Angew. Chem., Int. Ed.* **1999**, *38*, 1292. (e) Fukaya, K.; Yamase, T. *Angew. Chem., Int. Ed.* **2003**, *42*, 654. (f) Burkholder, E.; Zubieta, J. *Chem. Commun.* **2001**, 2056. (g) Hagrman, P. J.; Hagrman, D.; Zubieta, J. *Angew. Chem., Int. Ed.* **1999**, *38*, 2638.

(3) (a) Yamase, T. *Chem. Rev.* **1998**, *98*, 307. (b) Müller, A.; Shah, S. Q. N.; BPgge, H.; Schmidtmann, M. *Nature* **1999**, *397*, 48. (c) Xu, L.; Lu, M.; Xu, B.; Wei, Y.; Peng, Z.; Powell, D. R. *Angew. Chem., Int. Ed.* **2002**, *41*, 4129. (d) Chen, L.; Jiang, F.; Lin, Z.; Zhou, Y.; Yue, C.; Hong, M. *J. Am. Chem. Soc.* **2005**, *127*, 8588. (e) Kögerler, P.; Cronin, L. *Angew. Chem., Int. Ed.* **2005**, *44*, 844. (f) Coronado, E.; Gómez-García, C. J. *Chem. Rev.* **1998**, *98*, 273. (g) Wang, P.; Wang, X.; Zhu, G. *New J. Chem.* **2000**, *24*, 481. (h) Wang, P.; Wang, X.; Zhu, G. *Electrochim. Acta* **2000**, *46*, 637.

(4) (a) Eddaoudi, M.; Moler, D. B.; Li, H. L.; Chen, B. L.; Reineke, T. M.; O'Keeffe, M.; Yaghi, O. M. *Acc. Chem. Res.* **2001**, *34*, 319. (b) James, S. L. *Chem. Soc. Rev.* **2003**, *32*, 276.

(5) (a) Hagrman, D.; Zubieta, C.; Rose, D. J.; Zubieta, J.; Haushalter, R. C. *Angew. Chem., Int. Ed.* **1997**, *36*, 873. (b) Hagrman, D.; Hagrman, P. J.; Zubieta, J. *Angew. Chem., Int. Ed.* **1999**, *38*, 3165. (c) Ren, Y. P.; Kong, X. J.; Hu, X. Y.; Sun, M.; Long, L. S.; Huang, R. B.; Zheng, L. S. *Inorg. Chem.* **2006**, *45*, 4016. (d) Kong, X. J.; Ren, Y. P.; Zheng, P. Q.; Long, Y. X.; Long, L. S.; Huang, R. B.; Zheng, L. S. *Inorg. Chem.* **2006**, *45*, 10702. (e) Xu, Y.; Nie, L. B.; Zhu, D. R.; Song, Y.; Zhou, G. P.; You, W. S. *Cryst. Growth Des.* **2007**, *7*, 925. (f) Lu, J.; Shen, E. H.; Li, Y. G.; Xiao, D. R.; Wang, E. B.; Xu, L. *Cryst. Growth Des.* **2005**, *5*, 65. (h) Lan, Y. Q.; Li, S. L.; Su, Z. M.; Shao, K. Z.; Ma, J. F.; Wang, X. L.; Wang, E. B. *Chem. Commun.* **2008**, 58.

(6) (a) Streb, C.; Ritchie, C.; Long, D.-L.; Kögerler, P.; Cronin, L. *Angew. Chem., Int. Ed.* **2007**, *46*, 7579. (b) Song, Y.-F.; Long, D.-L.; Cronin, L. *Angew. Chem., Int. Ed.* **2007**, *46*, 3900.

(7) (a) Chen, X. M.; Tong, M. L. *Acc. Chem. Res.* **2007**, *40*, 162. (b) Zhang, J. P.; Chen, X. M. *Chem. Commun.* **2006**, 1689. (c) Zhang, J. P.; Zheng, S. L.; Huang, X. C.; Chen, X. M. *Angew. Chem., Int. Ed.* **2004**, *43*, 206. (d) Zhang, J. P.; Lin, Y. Y.; Huang, X. C.; Chen, X. M. *J. Am. Chem. Soc.* **2005**, *127*, 5495.

(8) (a) Lu, J. Y. *Coord. Chem. Rev.* **2003**, *246*, 327. (b) Zhang, X.-M. *Coord. Chem. Rev.* **2005**, *249*, 1201.

(9) Huang, X.-C.; Zhang, J.-P.; Lin, Y.-Y.; Chen, X.-M. *Chem. Commun.* **2004**, 1100.

(10) (a) Moulton, B.; Zaworotko, M. J. *Chem. Rev.* **2001**, *101*, 1629. (b) Blake, A. J.; Brooks, N. R.; Champness, N. R.; Crew, M.; Deveson, A.; Fenske, D.; Gregory, D. H.; Hanton, L. R.; Hubberstey, P.; Schröder, M. *Chem. Commun.* **2001**, 1432. (d) Barnett, S. A.; Blake, A. J.; Champness, N. R.; Wilson, C. *Chem. Commun.* **2002**, 1640. (e) Huang, X.-C.; Zhang, J.-P.; Lin, Y.-Y.; Chen, X.-M. *Chem. Commun.* **2005**, 2232. (f) Shin, D. M.; Lee, I. S.; Cho, D.; Chung, Y. K. *Inorg. Chem.* **2003**, *42*, 7722. (g) Chippindale, A. M.; Cheyne, S. M.; Hibble, S. J. *Angew. Chem., Int. Ed.* **2005**, *44*, 7942. (h) Bi, W.-H.; Cao, R.; Sun, D. F.; Yuan, D.-Q.; Li, X.; Wang, Y.-Q.; Li, X.-J.; Hong, M.-C. *Chem. Commun.* **2004**, 2104. (i) Fromm, K. M.; Doimeadios, J. L. S.; Robin, A. Y. *Chem. Commun.* **2005**, 4548.

(11) (a) Hennigar, T. L.; MacQuarrie, D. C.; Losier, P.; Rogers, R. D.; Zaworotko, M. J. *Angew. Chem., Int. Ed. Engl.* **1997**, *36*, 972. (b) Abourahma, H.; Moulton, B.; Kravtsov, V.; Zaworotko, M. J. *J. Am. Chem. Soc.* **2002**, *124*, 9990. (c) Huang, X.-C.; Zhang, J.-P.; Chen, X.-M. *J. Am. Chem. Soc.* **2004**, *126*, 13218. (d) Braga, D.; Curzi, M.; Grepioni, F.; Polito, M. *Chem. Commun.* **2005**, 2915. (e) Holmes, K. E.; Kelly, P. F.; Elsegood, M. R. J. *Dalton Trans.* **2004**, 3488. (f) Jiang, L.; Lu, T.-B.; Feng, X.-L. *Inorg. Chem.* **2005**, *44*, 7056.

(12) (a) Lan, Y. Q.; Li, S. L.; Wang, X. L.; Su, Z. M.; Shao, K. Z.; Wang, E. B. *Inorg. Chem.* **2008**, *47*, 529. (b) Li, S. L.; Lan, Y. Q.; Ma, J. F.; Yang, J.; Liu, J.; Fu, Y. M.; Su, Z. M. *Dalton Trans.* **2008**, 2015.

under hydrothermal conditions.[13] Et_3N is easy to control to build POM-based MOFs because it does not coordinate to the metal ion. (ii) Octamolybdates are an important branch in the polyoxomolybdate chemistry because of their varied structural patterns in the solid state. To date, eight isomeric forms of octamolybdates have been prepared, that is, α-isomer, *β*-isomer, *γ*-isomer, *δ*-isomer, *ε*-isomer, ζ-isomer, *η*-isomer, and *θ*-isomer.[14] As reported previously, the pH value of the reaction system is crucial for the formation of the above-mentioned isomers.[14a,15] Octamolybdate with a variety of structural isomers at different pH value may induce the formation of supramolecular isomers. (iii) The flexible bbi ligand, as a secondary N-donor ridging ligand, contains the flexible $-CH_2-$ spacer. Therefore, the two imidazole rings can freely twist around the $-CH_2-$ group to meet the requirements of the coordination geometries of metal atoms in the assembly process. Conformational changes of flexible ligands generate a different but often related network architecture, which often leads to supramolecular isomers,[9,10a] and can more easily produce these new classes of compounds. As accurate prediction of the final structures is impossible, we have tried different synthetic conditions and performed many experiments. Fortunately, compounds $[H_2bbi][Cu^{II}(bbi)_2(\beta\text{-}Mo_8O_{26})]$ (**1**), $[Cu^{II}(bbi)_2(H_2O)(\beta\text{-}Mo_8O_{26})_{0.5}]$ (**2**), $[Cu^{II}(bbi)_2(\alpha\text{-}Mo_8O_{26})][Cu^{I}(bbi)]_2$ (**3**), $[Cu^{II}Cu^{I}(bbi)_3(\alpha\text{-}Mo_8O_{26})][Cu^{I}(bbi)]$ (**4**), $[Cu^{I}(bbi)]_2[Cu^{I}_2(bbi)_2(\delta\text{-}Mo_8O_{26})_{0.5}][\alpha\text{-}Mo_8O_{26}]_{0.5}$ (**5**), and $[Cu^{I}(bbi)][Cu^{I}(bbi)(\theta\text{-}Mo_8O_{26})_{0.5}]$ (**6**) are successfully isolated by hydrothermal methods at different pH values. In addition, the infrared spectra, X-ray powder diffraction (XRPD), and thermogravimetric analyses have been investigated in detail for all compounds, and the luminescent properties have been also investigated for compounds **3** and **4**.

Experimental Section

Materials. All reagents and solvents for syntheses were purchased from commercial sources and used as received.

General Characterization and Physical Measurements. The C, H, and N elemental analyses were conducted on a Perkin-Elmer 240C elemental analyzer, and Mo and Cu were analyzed on a PLASMA-SPEC(I) ICP atomic emission spectrometer. The FT-IR spectra were recorded from KBr pellets in the range 4000−400 cm^{-1} on a Mattson Alpha-Centauri spectrometer. The XRPD patterns were recorded on a Siemens D5005 diffractometer with Cu KR (λ = 1.5418 Å) radiation. Thermogravimetric analyses (TGA) of the samples were performed on a Perkin-Elmer TG-7 analyzer heated from room temperature to 800 °C under nitrogen. Solid-state fluorescence spectra were recorded on a Cary Eclipse spectrofluorometer (Varian) equipped with a xenon lamp and quartz carrier at room temperature.

Syntheses of $[H_2bbi][Cu^{II}(bbi)_2(\beta\text{-}Mo_8O_{26})]$ (1). A mixture of $(NH_4)_6Mo_7O_{24}\cdot 4H_2O$ (0.124 g, 0.1 mmol), bbi (0.095 g, 0.5 mmol), $Cu(NO_3)_2\cdot 3H_2O$ (0.121 g, 0.5 mmol), and H_2O (10 mL) was adjusted to pH ≈ 1 with HNO_3 (1 M) and NaOH (1 M), stirred for 1 h, and then transferred and sealed in a 25 mL Teflon-lined stainless steel container, which was heated at 150 °C for 72 h and then cooled to room temperature at a rate of 10 °C·h^{-1}. Blue crystals of **1** were collected in 56.8% yield based on $Cu(NO_3)_2\cdot 3H_2O$. Elemental analyses calcd for $C_{30}H_{44}CuMo_8N_{12}O_{26}$ (1819.83): C, 19.80; H, 2.44; N, 9.24; Mo, 42.18; Cu, 3.49. Found: C, 19.89; H, 2.38; N, 9.34; Mo, 42.32; Cu, 3.51%. IR (cm^{-1}): 3217 (w), 1525 (m), 1444 (w), 1357 (w), 1241 (w), 1092 (m), 943 (s), 908 (s), 843 (s), 658 (s), 551 (m), 477 (m).

Syntheses of $[Cu^{II}(bbi)_2(H_2O)(\beta\text{-}Mo_8O_{26})_{0.5}]$ (2). The same synthetic procedure as that of **1** was used except for pH ≈ 3. Blue crystals of **2** were collected in 76.9% yield based on $Cu(NO_3)_2\cdot 3H_2O$. Elemental analyses calcd for $C_{20}H_{30}CuMo_4N_8O_{14}$ (1053.82): C, 22.79; H, 2.87; N, 10.63; Mo, 36.42; Cu, 6.03. Found: C, 22.83; H, 2.92; N, 10.73; Mo, 36.38; Cu, 5.99%. IR (cm^{-1}): 3731 (m), 3627 (w), 3118 (w), 1519 (m), 1439 (m), 1101 (w), 908 (s), 851 (s), 795 (s), 650 (s), 562 (m).

Synthesis of $[Cu^{II}(bbi)_2(\alpha\text{-}Mo_8O_{26})][Cu^{I}(bbi)]_2$ (3). A mixture of $(NH_4)_6Mo_7O_{24}\cdot 4H_2O$ (0.124 g, 0.1 mmol), bbi (0.095 g, 0.5 mmol), $Cu(NO_3)_2\cdot 3H_2O$ (0.121 g, 0.5 mmol), Et_3N (0.2 mL), and H_2O (10 mL) was adjusted to pH ≈ 2 with HNO_3 (1 M) and NaOH (1 M), stirred for 1 h, and then transferred and sealed in a 25 mL Teflon-lined stainless steel container, which was heated at 150 °C for 72 h and then cooled to room temperature at a rate of 10 °C·h^{-1}. Purple crystals of **3** were collected in 49.8% yield based on $Cu(NO_3)_2\cdot 3H_2O$. Elemental analyses calcd for $C_{40}H_{56}Cu_3Mo_8N_{16}O_{26}$ (2135.15): C, 22.50; H, 2.64; N, 10.50; Mo, 35.94; Cu, 8.93. Found: C, 22.63; H, 2.62; N, 10.43; Mo, 35.88; Cu, 8.99%. IR (cm^{-1}): 3438 (w), 3127 (w), 1588 (m), 1521 (m), 1438 (w), 1239 (m), 1104 (m), 956 (m), 922 (s), 797 (s), 656 (s), 561 (s).

Synthesis of $[Cu^{II}Cu^{I}(bbi)_3(\alpha\text{-}Mo_8O_{26})][Cu^{I}(bbi)]$ (4). The same synthetic procedure as that of **1** was used except for pH ≈ 4. Red crystals of **4** were collected in 63.1% yield based on $Cu(NO_3)_2\cdot 3H_2O$. Elemental analyses calcd for $C_{40}H_{56}Cu_3Mo_8N_{16}O_{26}$ (2135.15): C, 22.50; H, 2.64; N, 10.50; Mo, 35.94; Cu, 8.93. Found: C, 22.58; H, 2.58; N, 10.53; Mo, 35.98; Cu, 8.89%. IR (cm^{-1}): 3731 (w), 3117 (w), 1519 (m), 1439 (w), 1238 (w), 1100 (m), 908 (s), 794 (s), 649 (s), 560 (s), 499 (m).

X-ray Crystallography. Single-crystal X-ray diffraction data for compounds **1**−**6** were recorded on a Bruker Apex CCD diffractometer with graphite-monochromated Mo Kα radiation (λ = 0.71073 Å) at 293 K. Absorption corrections were applied using a multiscan technique. All the structures were solved by the Direct Method of SHELXS-97[16] and refined by full-matrix least-squares techniques using the SHELXL-97 program[17] within WINGX.[18] Non-hydrogen atoms were refined with anisotropic temperature parameters. The hydrogen atoms of the organic ligands were refined as rigid groups.

(13) (a) Shi, Z. Y.; Gu, X. J.; Peng, J.; Yu, X.; Wang, E. B. *Eur. J. Inorg. Chem.* **2006**, 385. (b) Shi, Z. Y.; Peng, J.; Gómez-García, C. J.; Gu, X. J. *J. Solid State Chem.* **2006**, *179*, 253. (c) Pavani, K.; Ramanan, A. *Eur. J. Inorg. Chem.* **2005**, 3080. (d) Pavani, K.; Lofland, S. E.; Ramanujachary, K. V.; Ramanan, A. *Eur. J. Inorg. Chem.* **2007**, 568.

(14) (a) Allis, D. G.; Rarig, R. G., Jr.; Burkholder, E.; Zubieta, J. *J. Mol. Struct.* **2004**, *688*, 11. (b) Bridgeman, A. J. *J. Phys. Chem. A* **2002**, *106*, 12151. (c) Allis, D. G.; Burkholder, E.; Zubieta, J. *Polyhedron* **2004**, *23*, 1145. (d) Wu, C. D.; Lu, C. Z.; Zhuang, H. H.; Huang, J. S. *Inorg. Chem.* **2002**, *41*, 5636. (e) Hagrman, D.; Zapf, P. J.; Zubieta, J. *Chem. Commun.* **1998**, 1283. (f) Xiao, D. R.; Hou, Y.; Wang, E. B.; Wang, S. T.; Li, Y. G.; Xu, L.; Hu, C. W. *Inorg. Chim. Acta* **2004**, *357*, 2525. (g) Rarig, R. S.; Zubieta, J. *Inorg. Chim. Acta* **2001**, *312*, 188.

(15) (a) Shi, Y. P.; Yang, W.; Xue, G. L.; Hu, H. M.; Wang, J. W. *J. Mol. Struct.* **2006**, *784*, 244. (b) Wang, W. J.; Xu, L.; Wei, Y. G.; Li, F. Y.; Gao, G. G.; Wang, E. B. *J. Solid State Chem.* **2005**, *178*, 608.

(16) Sheldrick, G. M. *SHELXS-97, Programs for X-ray Crystal Structure Solution*; University of Göttingen: Göttingen, Germany, 1997.

(17) Sheldrick, G. M. *SHELXL-97, Programs for X-ray Crystal Structure Refinement*; University of Göttingen: Göttingen, Germany, 1997.

(18) Farrugia, L. J. *WINGX, A Windows Program for Crystal Structure Analysis*; University of Glasgow: Glasgow, U.K., 1988.

Table 1. Crystal Data and Structure Refinements for Compounds **1**−**4**

	1	2	3	4
formula	$C_{30}H_{44}Cu$ $Mo_8N_{12}O_{26}$	$C_{20}H_{30}Cu$ $Mo_4N_8O_{14}$	$C_{40}H_{56}Cu_3$ $Mo_8N_{16}O_{26}$	$C_{40}H_{56}Cu_3$ $Mo_8N_{16}O_{26}$
fw	1819.83	1053.82	2135.15	2135.15
crystal system	triclinic	tetragonal	triclinic	triclinic
space group	$P\bar{1}$	$P\bar{4}$	$P\bar{1}$	$P\bar{1}$
a (Å)	11.3760(5)	14.3550(9)	12.2270(16)	11.698(2)
b (Å)	11.8230(5)	14.3550(9)	12.5960(17)	12.911(3)
c (Å)	11.8710(6)	16.474	12.9240(18)	13.001(3)
α (deg)	87.6040(10)	90	97.3260(10)	95.179(2)
β (deg)	67.5150(10)	90	111.837(2)	115.805(3)
γ (deg)	62.8610(10)	90	113.946(2)	112.281(2)
V (Å^3)	1295.64(10)	3394.7(3)	1595.0(4)	1557.1(5)
Z	1	4	1	1
$D_{calcd.}$ [g cm^{-3}]	2.332	2.062	2.223	2.277
F(000)	881	2060	1039	1039
reflns collected /unique	8011/5807	20929/8011	8196/5570	9508/6902
R(int)	0.0141	0.0895	0.0224	0.0226
GOF on F^2	1.047	0.986	1.058	1.059
R_1[a] [$I > 2\sigma(I)$]	0.0299	0.0590	0.0362	0.0580
wR_2[b]	0.0775	0.0928	0.0780	0.1300
largest residuals [e Å^{-3}]	1.402/−0.706	0.701/−0.553	1.112/−0.735	3.431/−3.697

[a] $R_1 = \sum||F_o| - |F_c||/\sum|F_o|$. [b] $wR_2 = |\sum w(|F_o|^2 - |F_c|^2)|/\sum|w(F_o^2)^2|^{1/2}$.

The hydrogen atoms of water molecules for compound **2** could not be positioned reliably. The detailed crystallographic data and structure refinement parameters are summarized in Table 1.

Results and Discussion

Structure Description of 1. Single-crystal X-ray structural analysis reveals that the structure of **1** contains two kinds of subunits, that is, protonated $(H_2bbi)^{2+}$ ligands and polymeric compostition $[Cu^{II}(bbi)_2(\beta\text{-}Mo_8O_{26})]^{2-}$, respectively. In the asymmetric unit (Figure 1a), there are one Cu^{II} cation and three bbi (bbi1, bbi2, and bbi3) ligands, and one $(\beta\text{-}Mo_8O_{26})^{4-}$ anion. The well-known $(\beta\text{-}Mo_8O_{26})^{4-}$ anion[15] consists of eight distorted corner- and/or edge-sharing {MoO6} octahedra. The $(\beta\text{-}Mo_8O_{26})^{4-}$ anion contains four kinds of O atoms, μ_5-O, μ_3-O, μ_2-O, and the terminal atoms (O_t). Each Cu^{II} cation is six coordinated by four nitrogen atoms (Cu−N = 1.990(4) Å, Supporting Information, Table S1) from four bbi ligands and two terminal oxygen atoms from different $(\beta\text{-}Mo_8O_{26})^{4-}$ anions (Cu−O = 2.732(4) Å) and shows a distorted octahedral coordination geometry. Three kinds of bbi ligands exhibit GTG (G = gauche and T = trans) conformations (Supporting Information, Table S2 and Figure S1a). Among them, bbi1 is dissociative and protonated by two H^+ ions. The bbi2 and bbi3 with bis-monodentate coordination modes link Cu^{II} cations to generate a 2D (4,4) sheet with the dimensions of 11.3 × 11.8 Å (Figure 1b and Supporting Information, Table S1b). Each $(\beta\text{-}Mo_8O_{26})^{4-}$ anion coordinates to two Cu^{II} cations from different sheets to form a 3D framework (Figure 1c). From the topological view, if each bbi and $(\beta\text{-}Mo_8O_{26})^{4-}$ can be considered as linkages, Cu^{II} cation is considered as a six-connected node, and the structure of **1** can be symbolized as a 6-connected framework with $(4^{12}\cdot6^3)$ topology (Figure 1d), which is a α-Po topology framework (Figure 1e).

It is interesting that each protonated bbi1 ligand acting as a counterion donates two hydrogen bonds to two terminal oxygen atoms from different $(\beta\text{-}Mo_8O_{26})^{4-}$ anions with the N···O distance of 2.938(7) Å, which makes bbi1 crystallize in the α-Po topology framework and stabilizes the ultimate structure further.

Structure Description of 2. When a different reaction pH value is selected, the interesting compound **2** is obtained. Single-crystal X-ray structural analysis reveals that there are two kinds of Cu^{II} cations, two kinds of bbi ligands, and one kind of $(\beta\text{-}Mo_8O_{26})^{4-}$ anion in the asymmetrical unit (Figure 2a). Cu1 and Cu2 are six-coordinated octahedral geometries which are surrounded by four nitrogen atoms from four bbi ligands and two terminal oxygen atoms for Cu1 (Cu(1)−N(1) = 1.948(12), Cu(1)−N(8) = 2.003(11), and Cu(1)−O(1) = 2.511(4) Å) and two water molecules for Cu2 (Cu(2)−N(3)#2 = 1.979(16), Cu(2)−N(5) = 1.996(16) and Cu(2)−O(1W) = 2.258(17) Å), respectively. Two kinds of bbi ligands exhibit TTT and GTG conformations (Supporting Information, Figure S2a) and coordinate to Cu^{II} cations to generate a 2D (4, 4) sheet (Figure 2b). Different from compound **1**, it shows the dimensional sizes of 12.8 × 13.3 Å (Supporting Information, Figure S2b), which may be due to different conformations of bbi ligands, and each $(\beta\text{-}Mo_8O_{26})^{4-}$ anion coordinates to two Cu^{II} cations with two terminal oxygen atoms to form an intricate 3D framework (Figures 2c and 2d). From the topological view, if each Cu1 is considered as a six-connected node, Cu2 acts as a four-connected node, and the bbi ligands as well as the $(\beta\text{-}Mo_8O_{26})^{4-}$ anion are considered as linkages. As a result, compound **2** shows a 3D (4,6)-connected framework with the $(4^4\cdot6^2)(4^4\cdot6^{10}\cdot8)$ topology.

The void space in the single framework is so large that two identical 3D frameworks interpenetrate each other to form a unique 2-fold interpenetration of the architecture (Figure 2e). In this structure, the longer internodes' linkers also play an essential role in constructing the 3D interpenetrated framework.

Structure Description of 3. X-ray diffraction analysis reveals that compound **3** contains two kinds of subunits, that

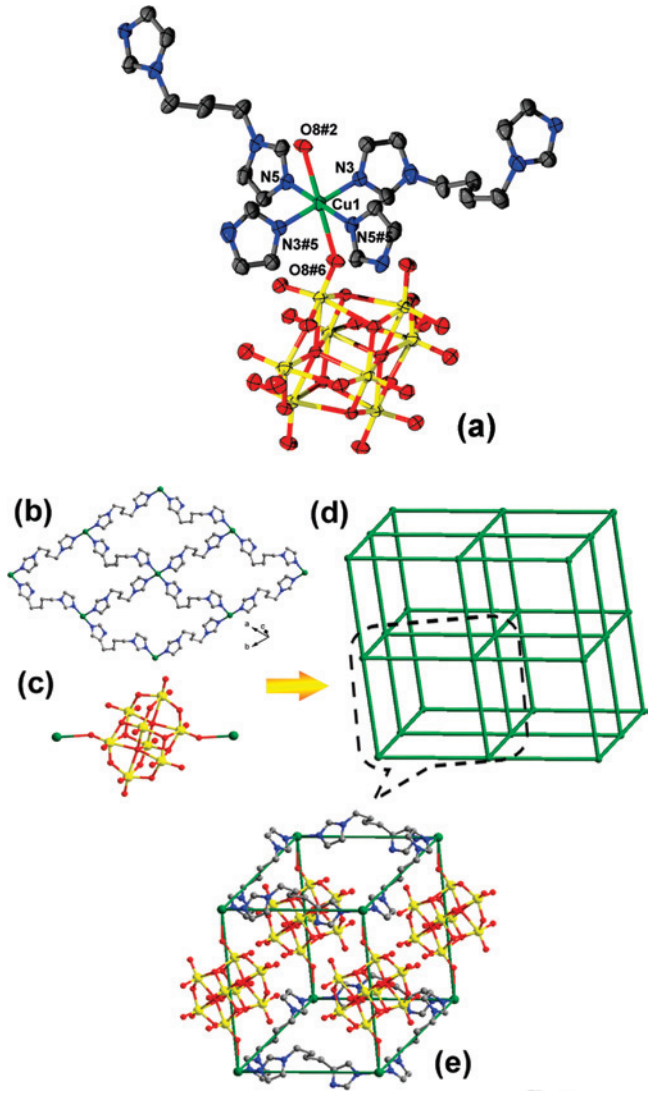

Figure 1. (a) Coordination environment of the Cu^{II} centers in compound **1** (all of the hydrogen atoms are omitted for clarity). (b) Ball-and-stick representation of the $(4^4,6^2)$ layerlike structure in **1**. (c) Ball-and-stick representation of the coordination mode of $(\beta\text{-}Mo_8O_{26})^{4-}$ anion. (d, e) Schematic view of the α-Po topology framework of **1**.

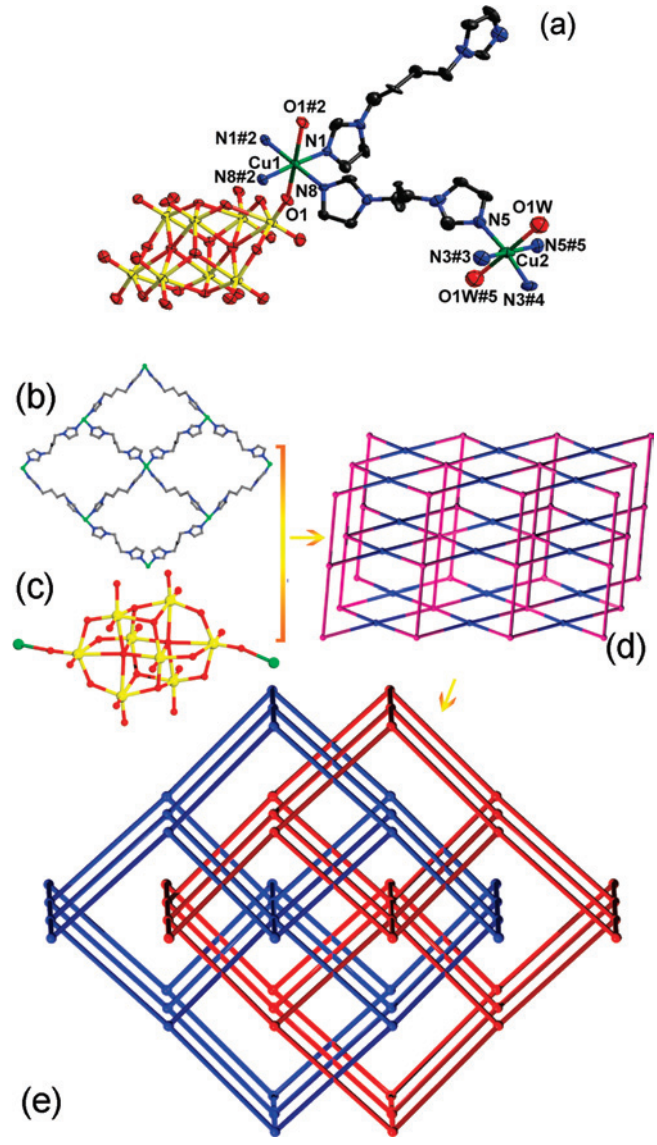

Figure 2. (a) Coordination environment of the Cu^{II} centers in compound **2** (all of the hydrogen atoms are omitted for clarity). (b) Ball-and-stick representation of the (4,4) sheet structure in **2**. (c) Ball-and-stick representation of the coordination mode of the $(\beta\text{-}Mo_8O_{26})^{4-}$ anion. (d) Schematic view of the 3D (4,6)-connected framework with the $(4^4\cdot6^2)(4^4\cdot6^{10}\cdot8)$ topology in **2** (pink and blue balls represent the 4 and 6-connected nodes, respectively). (e) Schematic view of the 2-fold interpenetrating structure of **2**.

is, $[Cu^{II}(bbi)_2(\alpha\text{-}Mo_8O_{26})]^{2-}$ and $[Cu^{I}(bbi)]^{+}$. There are two kinds of Cu^{II} and Cu^{I} cations, three kinds of bbi ligands, and one kind of $(\alpha\text{-}Mo_8O_{26})^{4-}$ anion (Figure 3a). In this case, Cu1 is a six-coordinated octahedral geometry which is completed by four nitrogen atoms from different bbi ligands and two terminal oxygen atoms (Cu(1)−N(2) = 1.959(4), Cu(1)−N(3) = 2.038(4), and Cu(1)−O(8) = 2.605(4) Å) from two $(\alpha\text{-}Mo_8O_{26})^{4-}$ anions. Cu2 exhibits closely line coordination geometry formed by two nitrogen atoms (Cu(2)−N(6) = 1.864(5) and Cu(2)−N(8)#6 = 1.863(5) Å) from two bbi ligands. Three kinds of bbi ligands show bis-monodentate coordination modes. The bbi1 and bbi2 with the TGT and TTT conformations (Supporting Information, Figure S3a) link Cu^{II} cations to generate a 2D (4,4) sheet (Figure 3b) with the dimensions of 13.5 × 14.1 Å (Supporting Information, Figure S3b), and each $(\alpha\text{-}Mo_8O_{26})^{4-}$ anion links two Cu^{II} cations (Figure 3c) from different layers to form a 3D α-Po topology framework (Figure 3d). The bbi3 ligands with TTT conformations form a $[Cu^{I}(bbi)]^{+}$ chain combined with Cu^{I} cations. As a result, the unusual 3D polythreaded framework is formed by two chains threading through the distorted α-Po skeleton. To further study the structure, if $Cu^{I}\cdots O$ interactions are considered, each Cu^{I} cation has $Cu^{I}\cdots O$ interactions with one terminal oxygen atom (Cu(2)−O(13) = 2.685(4) Å) from different $(\alpha\text{-}Mo_8O_{26})^{4-}$ anions, and each $(\alpha\text{-}Mo_8O_{26})^{4-}$ anion links two Cu^{II} and two Cu^{I} cations (Figure 3e), so the $[Cu^{I}(bbi)]^{+}$ chain is fixed in the α-Po skeleton. From the topological view, if each Cu^{II} cation is considered as a six-connected node, $(\alpha\text{-}Mo_8O_{26})^{4-}$ anion acts as a four-connected node, Cu^{I} cation is a three-connected node, and bbi ligands are considered as linkages, and so the structure of **3** is a novel self-penetrating (3,4,6)-connected framework with $(5^2\cdot8)_2(5^4\cdot6\cdot8)(4^4\cdot6^{10}\cdot10)$ topology (Figures 3f and 3g).

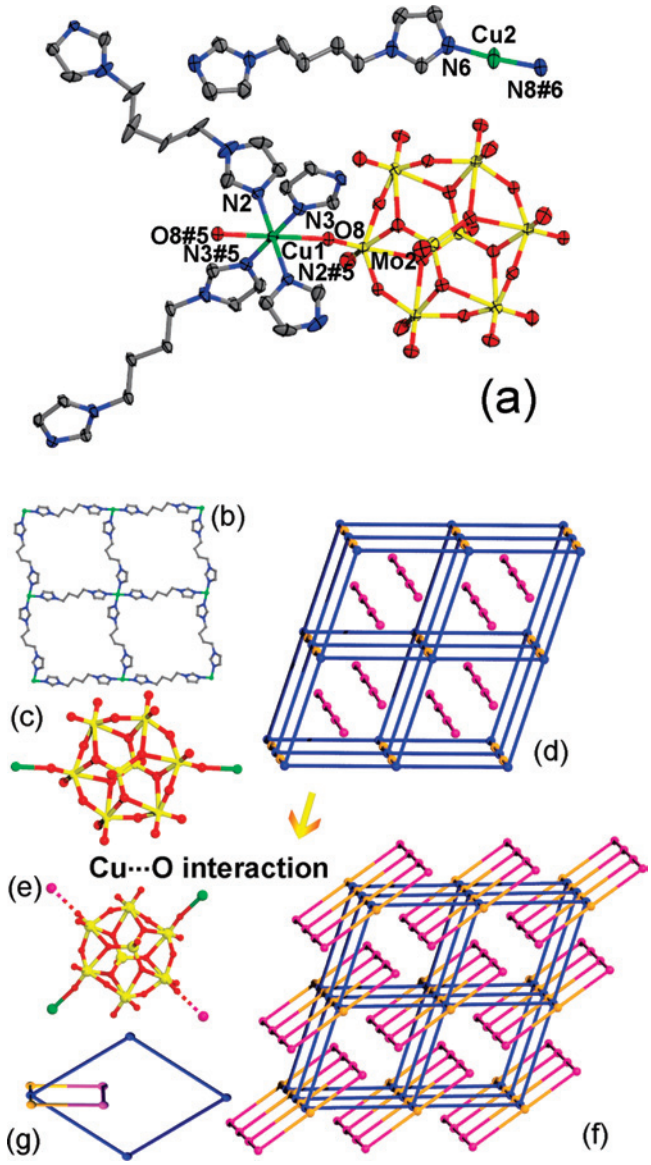

Figure 3. (a) Coordination environment of the $Cu^{I,II}$ centers in compound **3** (all of the hydrogen atoms are omitted for clarity). (b) Ball-and-stick representation of the (4,4) layerlike structure in **3**. (c) Ball-and-stick representation of the coordination mode of the $(\beta\text{-}Mo_8O_{26})^{4-}$ anion. (d) Schematic view of the 3D polythreaded framework of **3**. (e) Ball-and-stick representation of the coordination mode of the $(\alpha\text{-}Mo_8O_{26})^{4-}$ anion (the $Cu^I\cdots O$ interactions being considered). (f, g) The self-penetrating (3,4,6)-connected framework with $(5^2\cdot8)_2(5^4\cdot6\cdot8)(4^4\cdot6^{10}\cdot10)$ topology in **3** (pink, yellow, and blue balls represent the 3, 4, and 6-connected nodes, respectively).

The entangled system has been defined by Ciani and coworkers, which includes interpenetration, polycatenation, polythreading, polyknotting, and so on.[19] Polythreaded structures are characterized by the presence of closed loops, as well as the elements that can thread through the loops, and can be considered as extended periodic analogues of molecular rotaxanes and pseudorotaxanes. Self-penetrating (self-catenation or polyknotting) frameworks are single nets having the peculiarity that the smallest topological rings catenated by other rings belong to the same network. Compound **3** represents two different entangled frameworks whether the $Cu^I\cdots O$ interaction is considered or not. Hitherto, a few self-penetrated nets have been observed in MOFs.[20] However, the POMs-based self-penetrating framework has not been observed. Compound **3** represents the first example of a self-penetrating framework presently known for the octamolybdate systems.

Structure Description of 4. Similar to compound **3**, there are two kinds of subunits in the asymmetrical unit, that is, $[Cu^{II}Cu^I(bbi)_3(\alpha\text{-}Mo_8O_{26})]^-$ and $[Cu^I(bbi)]^+$. There are two kinds of Cu^I, one kind of Cu^{II} cation, three kinds of bbi ligands, and one kind of $(\alpha\text{-}Mo_8O_{26})^{4-}$ anion (Figure 4a). Cu^{II} exhibits a six-coordinated octahedral geometry which is surrounded by four nitrogen atoms (Cu(1)−N(7) = 2.000(12) and Cu(1)−N(1) = 2.016(8) Å) from different bbi ligands and two terminal oxygen atoms (Cu(1)−O(4) = 2.556(7) Å) from different $(\alpha\text{-}Mo_8O_{26})^{4-}$ anions. Cu^I2 and Cu^I3 show closely line geometries which are completed by two nitrogen atoms (Cu(2)−N(5) = 1.899(7) and Cu(3)−N(4) =1.909(7) Å) from different bbi ligands. Three kinds of bbi ligands exhibit GTT, TTT, and GTG conformations (Supporting Information, Figure S4a). The bbi1 and bbi3 link Cu1 and Cu3 cations to generate a 2D (4,4) sheet (Figure 4b), which contains a large 66-membered ring (Supporting Information, Figure S4b). Each $(\alpha\text{-}Mo_8O_{26})^{4-}$ anion coordinates to two Cu^{II} cations (Figure 4c) from different sheets to form a 3D framework. From the topological view, if each Cu^{II} cation is considered as a six-connected node, Cu3 cation, $(\alpha\text{-}Mo_8O_{26})^{4-}$ anion, and bbi ligand are considered as linkages, the structure is a 6-connected framework with the α-Po topology, and the bbi2 ligand and Cu2 cation form a $[Cu^I(bbi)]^+$ chain which threads through the above 3D framework. As a result, compound **4** shows the unusual 3D polythreaded framework (Figure 4d). If $Cu^I\cdots O$ interactions are considered, each Cu^I cation has $Cu^I\cdots O$ interactions with two terminal oxygen atoms (Cu(2)−O(7) = 2.742(4) and Cu(3)−O(2) = 2.754(4) Å) from different $(\alpha\text{-}Mo_8O_{26})^{4-}$ anions, and each $(\alpha\text{-}Mo_8O_{26})^{4-}$ anion links two Cu^{II} and four Cu^I cations (Figure 4e), so the $[Cu^I(bbi)]^+$ chain is fixed in the 3D skeleton. From the topological view, if each Cu^{II} cation and $(\alpha\text{-}Mo_8O_{26})^{4-}$ anion are considered as six-connected nodes; Cu2 and Cu3 cations act as two kinds of four-connected nodes, and bbi ligands are considered as linkers; the structure of **4** is a (4,6)-connected framework with $(4^2\cdot6^3\cdot7)(5\cdot6^4\cdot8)(4^2\cdot5^6\cdot6^6\cdot8)(4^2\cdot5^6\cdot6^4\cdot7\cdot8^2)$ topology (Figure 4f).

(19) (a) Carlucci, L.; Ciani, G.; Proserpio, D. M. *Coord. Chem. Rev.* **2003**, *246*, 247. (b) Batten, S. R.; Robson, R. *Angew. Chem., Int. Ed.* **1998**, *37*, 1460. (c) Carlucci, L.; Ciani, G.; Proserpio, D. M. *CrystEngComm* **2003**, *5*, 269. (d) Bu, X. H.; Tong, M. L.; Chang, H. C.; Kitagawa, S.; Batten, S. R. *Angew. Chem., Int. Ed.* **2004**, *43*, 192. (e) Liang, K.; Zheng, H.; Song, Y.; Lappert, M. F.; Li, Y.; Xin, X.; Huang, Z.; Chen, J.; Lu, S. *Angew. Chem., Int. Ed.* **2004**, *43*, 5776. (f) Wang, X. L.; Qin, C.; Wang, E. B.; Li, Y. G.; Su, Z. M.; Xu, L.; Carlucci, L. *Angew. Chem., Int. Ed.* **2005**, *44*, 5824.

(20) (a) Wang, X. L.; Qin, C.; Wang, E. B.; Su, Z. M.; Xu, L.; Batten, S. R. *Chem. Commun.* **2005**, 4789. (b) Wang, X. L.; Qin, C.; Wang, E. B.; Su, Z. M. *Chem.—Eur. J.* **2006**, *12*, 2680. (c) Carlucci, L.; Ciani, G.; Proserpio, D. M.; Porta, F. *Angew. Chem., Int. Ed.* **2003**, *42*, 317. (d) Li, X.; Cao, R.; Sun, D. F.; Bi, W. H; Yuan, D. Q. *Eur. J. Inorg. Chem.* **2004**, 2228. (e) Lan, Y. Q.; Li, S. L.; Wang, X. L.; Su, Z. M.; Shao, K. Z.; Wang, E. B. *Chem. Commun.* **2007**, 4863. (f) Zhang, J.; Yao, Y. G.; Bu, X. H. *Chem. Mater.* **2007**, *19*, 5083. (g) Qu, X. S.; Xu, L.; Gao, G. G.; Li, F. Y.; Yang, Y. Y. *Inorg. Chem.* **2007**, *46*, 4775.

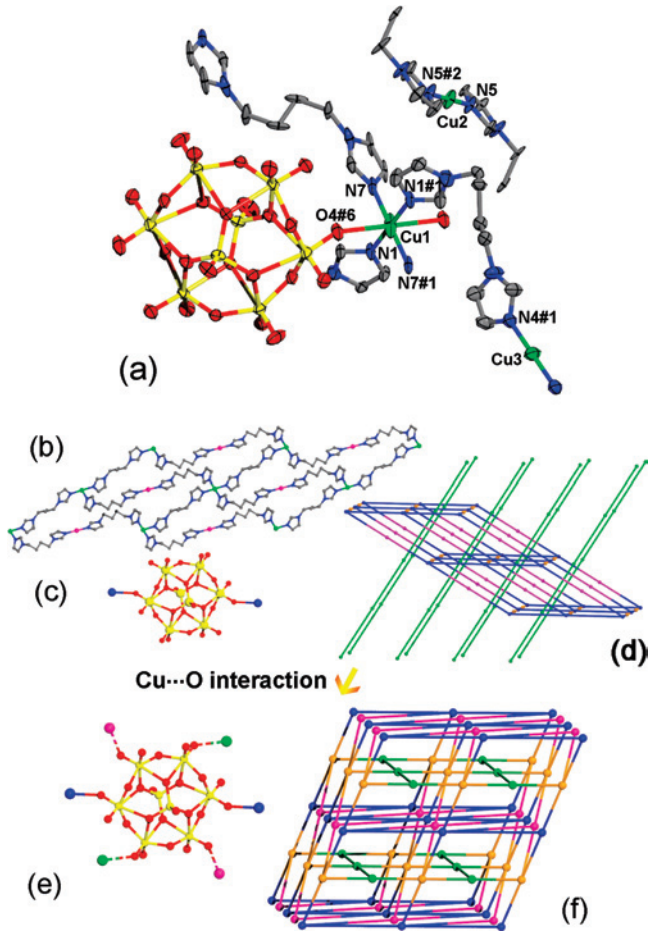

Figure 4. (a) Coordination environment of the $Cu^{I,II}$ centers in compound **4** (all of the hydrogen atoms are omitted for clarity). (b) Ball-and-stick representation of the $(4^4,6^2)$ layerlike structure in **4**. (c) Ball-and-stick representation of the coordination mode of $(\beta\text{-}Mo_8O_{26})^{4-}$ anion. (d) Schematic view of the 3D polythreaded framework of **4**. (e) Ball-and-stick representation of the coordination mode of the $(\alpha\text{-}Mo_8O_{26})^{4-}$ anion (the $Cu^I\cdots O$ interactions being considered). (f) Schematic view of the (4,6)-connected framework with $(4^2\cdot6^3\cdot7)(5\cdot6^4\cdot8)(4^2\cdot5^6\cdot6^6\cdot8)(4^2\cdot5^6\cdot6^4\cdot7\cdot8^2)$ topology in **4** (pink and green balls represent the two kinds of 4-connected nodes, respectively, and yellow and blue ones represent the two kinds of 6-connected nodes, respectively).

Offering further insight into the structures of **3** and **4**, they are supramolecular isomers. If the $Cu^I\cdots O$ interactions are not considered, they show two different polythreaded frameworks. In **3**, along the special axis (u, v, w: 1, 1, 1 or h, k, l: 2.04, 5.45, 6.33), two $[Cu^I(bbi)]^+$ chains penetrate the distorted α-Po topology framework, which is constructed from $(\alpha\text{-}Mo_8O_{26})^{4-}$ anions linking (4,4) sheets of $[Cu^I_4(bbi)]^{2+}$ units (Supporting Information, Figure S5a). In **4**, (4,4) sheets formed by bbi ligands, Cu^{II}, and Cu^I cations are pillared by $(\alpha\text{-}Mo_8O_{26})^{4-}$ to generate a distorted α-Po topology framework. Different from **3**, only one kind of $[Cu^I(bbi)]^+$ chain penetrates the distorted α-Po topology framework in an inclined way along the *c* axis to construct the other polythreaded framework (Supporting Information, Figure S5b). The successful isolation of **3** and **4** may provide a valuable clue for the supramolecular isomerism, which helps to understand the structure−property relationship of POMs-based MOFs.

Structure Description of 5 and 6. The structures of these two complexes have been reported in our previous article.[12a] The simple descriptions will be given in this section for the convenience of comparison with other compounds. They are supramolecular isomers with polythreaded topology based on octamolybdate isomers. There are two kinds of octamolybdates, $(\alpha\text{-}Mo_8O_{26})^{4-}$and $(\delta\text{-}Mo_8O_{26})^{4-}$, in compound **5**. $(\delta\text{-}Mo_8O_{26})^{4-}$ as a linker and $(\alpha\text{-}Mo_8O_{26})^{4-}$ as a 4-connected node link $[Cu^I(bbi)]^+_\infty$ unit by covalent connection and $Cu^I\cdots O$ interaction form a 2D sheet, respectively. The other $[Cu^I(bbi)]^+_\infty$ chain penetrates the 2D sheet along the crystallographic *b* axis to form the polythreaded structure (Supporting Information, Figure S6a). In compound **6**, $(\theta\text{-}Mo_8O_{26})^{4-}$ polyanions coordinate to two Cu^I from adjacent $[Cu^I(bbi)]^+_\infty$ monochains to generate a ladderlike double-chain along the crystallographic *c* axis by covalent connection. The other $[Cu^I(bbi)]^+_\infty$ chains penetrate the ladderlike double-chain in an inclined way to form the polythreaded structure. In the two compounds we can find the occurrence of cuprophilic interaction,[21] which enhances the stabilization of the frameworks (Supporting Information, Figure S6b). Comparing the structure of **5** with **6**, if the θ-isomer substitutes the α-isomer and δ-isomer, isomer **5** exhibits the same structural type with **6**. The difference between isomers **5** and **6** arises essentially from octamolybdate isomers. The ocatmolybdate isomers maybe play crucial roles in the formation of supramolecular isomerism.

Syntheses of the Compounds. In compounds **1** and **2**, Cu cations show the valence of +2 without Et_3N. The presence of Cu^{II} and Cu^I in compounds **3** and **4** indicates that the starting Cu^{II} ions are reduced by organic amine compositions partially. With step by step increase of the amount of Et_3N, Cu^{II} ions transform into Cu^I ones completely in compounds **5** and **6**. We have achieved the transformation of Cu^{II} ions into Cu^I ones in different degrees by changing the amount of organic amine in POMs-based MOFs for the first time. These results indicate that the Cu^{II} cations can be easily reduced to Cu^I cations by organic amine (Et_3N in this paper), in a similar manner as in a previous investigation of in situ hydrothermal reactions.[13]

At the same time, the different reaction pH values have an influence on the formation of final products. When the same raw starting materials are selected, different compounds are isolated at pH ≈ 1 for **1** and 3 for **2**, respectively. The same change occurs in compounds **3** (pH ≈ 2) and **4** (pH ≈ 4), and **5** (pH ≈ 5) and **6** (pH ≈ 2). It is interesting that compounds **3** and **4**, and **5** and **6**, are supramolecular isomers, respectively. However, most of the exact mechanisms of the formation of a supramolecular isomer are not yet well-proven. Compared with compounds **1** and **2**, in synthesizing **3**−**6**, organic amine may be plays an important effect on supramolecular isomerism. The function of organic amine may be not only as a reducer but also as buffering agent to reduce the crystallization speed, which favors forming the similar products (such as supramolecular isomers, Scheme 1).

(21) (a) Pyykkö, P. *Chem. Rev.* **1997**, *97*, 597. (b) Khlobystov, A. N.; Blake, A. J.; Champness, N. R.; Lemenovskii, D. A.; Majouga, A. G.; Zyk, N. V.; Schröder, M. *Coord. Chem. Rev.* **2001**, *222*, 155. (c) Che, C. M.; Mao, Z.; Miskowski, V. M.; Tse, M. C.; Chan, C. K.; Cheung, K. K.; Phillips, D. L.; Leung, K. H. *Angew. Chem., Int. Ed.* **2000**, *39*, 4084.

Scheme 1. Schematic View of the Syntheses of Compounds **1**−**6** in This Work[a]

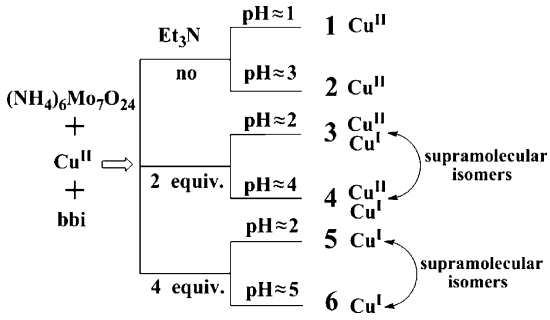

[a] equiv. = equivalent.

Self-Assembly of the Compounds. According to previous research, the coordination ability of the nitrogen atom from the organic ligand is stronger than of the polyanion and water.[22] In compounds **1**−**6**, each copper cation is first coordinated by nitrogen atoms from bbi ligands to form various Cu−bbi metal-organic units. The Cu^{II}-bbi units show (4,4) sheets in **1**−**3** and Cu^{I}-bbi units display chains in **3**−**6**. It is interesting that the (4,4) sheet is formed by Cu^{II}, Cu^{I}, and bbi in **4**. Simultaneously, various octamolybdate isomers are aggregates of $(Mo_7O_{24})^{6-}$ polyanions under different reaction conditions. So the above-mentioned Cu−bbi metal-organic units and various octamolybdate isomers in aqueous solution self-assemble to crystallize different solid products by hydrolysis and condensation reactions from previous research.[13d] For **1**, $(\beta\text{-}Mo_8O_{26})^{4-}$ clusters connect Cu^{II}-bbi units to form a α-Po net, in which it co-crystallizes the protonated $(H_2bbi)^{2+}$ ligands at lower pH value (pH ≈ 1) for charge balance. When at higher pH value (pH ≈ 3) in **2**, $(\beta\text{-}Mo_8O_{26})^{4-}$ clusters and water molecules coordinate to Cu^{II}-bbi units to product a 2-fold (4,6)-connected framework. The difference between **1** and **2** may be due to the ability of bbi of getting protons and the coordination ability of water molecules at different pH values. In **3** and **4**, the polar sites of Cu^{II} cations are coordinated by $(\alpha\text{-}Mo_8O_{26})^{4-}$ clusters, so $(\alpha\text{-}Mo_8O_{26})^{4-}$ clusters and different (4,4) layers are self-assembled to give α-Po nets. Then, the Cu^{I}-bbi units co-crystallize in the above-mentioned nets through nonbonding ($Cu^{I}\cdots O$) interactions. For **5** and **6**, different $(Mo_8O_{26})^{4-}$ isomers connect some Cu^{I}-bbi chains to form two kinds of ladderlike double-chains. Then, the other Cu^{I}-bbi chains thread the ladderlike double-chains and form **5** and **6** by nonbonding interactions ($Cu^{I}\cdots O$ and cuprophilic interactions in **5** and in **6**). Comparing the structure of **5** with **6**, the difference arises essentially from various octamolybdate isomers which are aggregated from acidified aqueous molybdate solution at different pH values.

On the basis of above discussion, crystal packings of **1**−**6** are a balance of several forces, such as redox chemistry (the quantity of Et_3N), acid−base chemistry (the different pH values), the coordination ability and species of ions (cations and anions), the structural types of coppe-bbi units, and nonbonding interactions ($Cu^{I}\cdots O$ and/or cuprophilic interactions).

Effect of the Copper-bbi Units and the Types and Coordination Modes of Polyanions on the Structures. Unambiguously, the different copper-bbi units and the coordination modes of polyanions have significant effects on the final structure of compounds **1**−**6**. Because of the strong Jahn−Teller effect of the d^9 electronic configuration, Cu^{II} cation tends to form the elongated octahedral coordination geometry with 6 coordination numbers. Cu^{I} ion prefers a linear, "T-shaped", or distorted tetrahedron coordination geometry with 2−4 coordination numbers. So Cu^{II} cations are coordinated by four bbi ligands in the equatorial sites, and Cu^{II} cations are coordinated by two bbi ligands to form different copper-bbi units. These copper-bbi units with polyanions co-crystallize to form different compounds. In **1** and **2**, polyanions show $(\beta\text{-}Mo_8O_{26})^{4-}$ clusters which coordinate to two Cu^{II} cations from different Cu^{II}-bbi sheets to generate two kinds of 3D structures. In **3** and **4**, polyanions show $(\alpha\text{-}Mo_8O_{26})^{4-}$ clusters which coordinate to two Cu^{II} cations to generate α-Po nets, and $(\alpha\text{-}Mo_8O_{26})^{4-}$ clusters connect two Cu^{I} cations in **3** and four Cu^{I} in **4** by $Cu^{I}\cdots O$ interactions to form different 3D topological frameworks. There are $(\delta\text{-}Mo_8O_{26})^{4-}$ and $(\alpha\text{-}Mo_8O_{26})^{4-}$ polyanions in **5**, in which $(\delta\text{-}Mo_8O_{26})^{4-}$ coordinates two Cu^{I} ions and $(\alpha\text{-}Mo_8O_{26})^{4-}$ acts as a counterion. When $Cu^{I}\cdots O$ interactions are considered, $(\alpha\text{-}Mo_8O_{26})^{4-}$ link four Cu^{I} cations to generate a 2D polythreaded structure. In **6**, $(\theta\text{-}Mo_8O_{26})^{4-}$ cluster coordinates to two Cu^{I} cations to form the other polythreaded structure. So it can be seen that the coordination behaviors and types of $(Mo_8O_{26})^{4-}$ polyanions have great influences on the frameworks of the complexes (Scheme 2).

The results indicate that various copper-organic units which are formed by bbi ligands combined with Cu^{II}/Cu^{I} cations, octamolybdates with different isomers and coordination modes, and the interactions between polyanions and copper-organic units are important for the formation of the different structures for **1**−**6**.

Thermal Analysis. The thermogravimetric analysis (TGA) experiments were performed under a N_2 atmosphere with a heating rate of 10 °C·min^{-1} in temperatures ranging from room temperature to 800 °C shown in Supporting Information, Figure S7. To characterize the compounds more fully in terms of thermal stability, we have examined compounds **1**−**4** using TGA. The TGA curve of compound **1** shows a weight loss of 10.3% from room temperature to 159 °C, corresponding to the release of uncoordinated bbi ligand (calcd 10.4%). The residual composition begins to decompose at 308 °C and ends above 678 °C. The TG curve of compound **2** shows a weight loss of 1.5% from room temperature to 182 °C, corresponding to the release of one coordinated water molecule (calcd 1.7%). The anhydrous composition begins to decompose at 253 °C and ends above 559 °C. The anhydrous compounds **3** and **4** begin to decompose at 319 and 317 °C and end above 700 and 692 °C, respectively.

(22) (a) Li, S. L.; Lan, Y. Q.; Ma, J. F.; Yang, J.; Wang, X. H.; Su, Z. M. *Inorg. Chem.* **2007**, *46*, 8283. (b) Ramanan, A.; Whittingham, M. S. *Cryst. Growth Des.* **2006**, *6*, 2419.

Scheme 2. Schematic View of Six Compounds in This Work

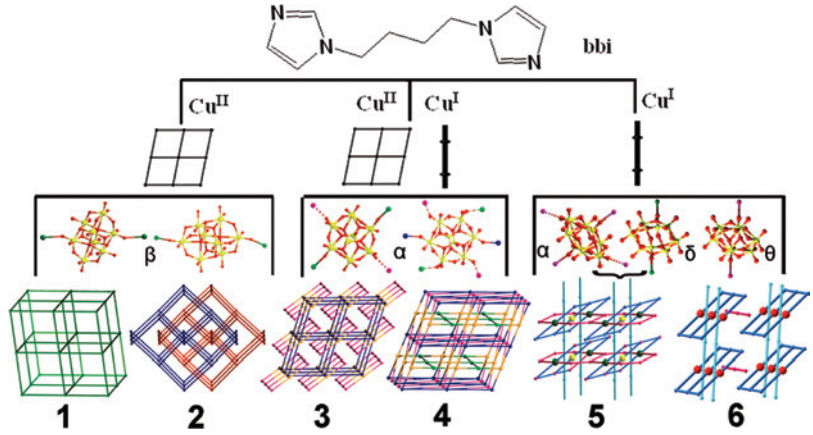

XRPD Patterns. The XRPD patterns for compounds **1**−**4** are presented in Supporting Information, Figure S8. The diffraction peaks of both simulated and experimental patterns match well in key positions, indicating thus the phase purities of compounds **1**−**4**.

Luminescent Properties. Luminescent compounds are of great current interest because of their various applications in chemical sensors, photochemistry, and electroluminescent display.[23] The photoluminescent properties of compounds **3** and **4** were studied at room temperature (Supporting Information, Figure S9). It can be observed that the maximum emission wavelength occurs at 362 nm (λ_{ex} = 300 nm) for **3**, 365 nm (λ_{ex} = 300 nm) for **4**, 364 nm (λ_{ex} = 300 nm) for **5**, and 377 nm (λ_{ex} = 300 nm) for **6**,[12a] which are blue-shifted compared with that of pure bbi ligand (λ_{em} = 438 nm, λ_{ex} = 300 nm).[24] The minor differences among **3**−**6** may be caused by neutral ligands with different coordination conformations. The origin of the emission for compounds **3**−**6** might be attributable to ligand-to-metal charge transfer and/or the intraligand ($\pi^* \rightarrow \pi$) fluorescent emission.[25] This implies that these complexes could be potentially used as luminescent materials.

Conclusion

In conclusion, we have designed and synthesized six POM-based hybrid materials based on octamolybdate building blocks and copper-organic units at different pH values under hydrothermal conditions. It is infrequent that compounds **3** and **4**, and **5** and **6**, are supramolecular isomers in POMs-based MOFs, respectively. By careful inspection of the structures of **1**−**6**, we believed that various copper-organic units which are formed by bbi ligands combined with Cu^{II}/Cu^{I} cations, octamolybdates with different types and coordination modes, and the nonbonding interactions between polyanions and copper-organic units are important for the formation of the different structures. With step by step increase of the amount of organic amine, we have achieved the transformation of Cu^{II} ions into Cu^{I} ones in different degrees in POMs-based MOFs for the first time. The function of organic amine may be not only as a reducer but also as a buffering agent to reduce the crystallization speed, which is in favor of forming the similar products (such as supramolecular isomers). The successful isolation of these species maybe will provide a calculable clue for the supramolecular isomerism in POMs-based MOFs, which may help to understand the structure−property relationship of POMs-based MOFs. Further research is ongoing to prepare novel supramolecular isomers and explore their valuable properties. More importantly, the combination of these three important research fields, namely, in situ synthesization, supramolecular isomerism, and polyoxometalate chemistry, opens up new possibilities in pursuit of multifunctional materials.

Acknowledgment. The authors gratefully acknowledge the financial support from the National Natural Science Foundation of China (Project Nos. 20573016 and 20703008), the National High-tech Research and Development Program (863 Program 2007AA03Z354), Program for Changjiang Scholars and Innovative Research Team in University (IRT0714), and the Science Foundation for Young Teachers of Northeast Normal University (No. 20070309).

Supporting Information Available: Crystallographic data in CIF format and additional figures, selected bond distances, TGA, XRPD, luminescent spectrum and EPR in PDF format. This material is available free of charge via the Internet at http://pubs.acs.org.

IC800702D

(23) (a) McGarrah, J. E.; Kim, Y.-J.; Hissler, M.; Eisenberg, R. *Inorg. Chem.* **2001**, *40*, 4510. (b) Wu, Q.; Esteghamatian, M.; Hu, N.-X.; Popovic, Z.; Enright, G.; Tao, Y.; D'Iorio, M.; Wang, S. *Chem. Mater.* **2000**, *12*, 79. (c) Santis, G. D.; Fabbrizzi, L.; Licchelli, M.; Poggi, A.; Taglietti, A. *Angew. Chem., Int. Ed. Engl.* **1996**, *35*, 202.

(24) (a) Liu, Y. Y.; Ma, J. F.; Yang, J.; Su, Z. M. *Inorg. Chem.* **2007**, *46*, 3027. (b) Li, S. L.; Lan, Y. Q.; Ma, J. F.; Yang, J.; Wei, G. H.; Zhang, L. P.; Su, Z. M *Cryst. Growth Des.* **2008**, *8*, 675.

(25) Luo, J. H.; Hong, M. C.; Wang, R. H.; Shi, Q.; Cao, R.; Weng, J. B.; Sun, R. Q.; Zhang, H. H. *Inorg. Chem. Commun.* **2003**, *6*, 702.